1-1-2007

Synthesis and Solid State ^{19}F-NMR Studies on Fluorine-labeled Antimicrobial Peptide RK-21

Mahender Budarapu

Synthesis and solid state ^{19}F-NMR studies on fluorine-labeled antimicrobial peptide RK-21

by

Mahender Budarapu

Thesis

Submitted to the Department of Chemistry

Eastern Michigan University

In partial fulfillment of the requirements

for the degree of

MASTER OF SCIENCE

in

Chemistry

December, 2007

Ypsilanti, Michigan.

DEDICATION

To

My family and friends

ACKNOWLEDGEMENTS

I would like to express my sincere gratitude to my research advisor Dr. Deborah Heyl-Clegg. Her continuous support and encouragement helped me a lot for the present thesis.

I deeply express my gratitude to my committee members, Dr. Steven Pernecky and Dr. Hedeel Evans.

I express my sincere gratitude to Dr. Krishnaswamy Rengan, who supported my stay at EMU, pointing me in the right direction.

I would like to thank the Head of Department, Dr. Ross Nord for his support and timely help. I would also like to thank the entire faculty who have taken pains to teach me new skills. I would like to thank all the members of Chemistry Department especially Brain Samuels, Carol Orlowski and Carolyn Jackson for their continuous support.

I would like to thank Dr Ramamoorthy, and Dr Ulli for their support. I would also wish to thank NIH grant AI054515 (Dr Ramamoorthy).

I would also wish to thank all my friends, classmates and all others who made my stay at EMU more fun.

Abstract

Antimicrobial peptides act against bacteria by binding non-specifically and disrupting their outer membrane. LL-37 is the only member of the cathelicidin group of antimicrobial peptides present in humans and shows a broad range of antimicrobial activity. RK-21 is a fragment of human antimicrobial peptide LL-37, which is α-helical, cationic and amphipathic in nature. RK-21 displays similar antimicrobial activity to LL-37. In order to understand the mechanism of lipid bilayer disruption, fluorine-labeled antimicrobial peptide RK-21 was chemically synthesized and ^{19}F-NMR studies were done. NMR studies were done at various peptide concentrations, on different lipid bilayer compositions and temperatures. ^{31}P-NMR studies did not show any micellar fragments, eliminating the detergent-like mechanism for activity. ^{19}F-NMR studies indicated that labeled RK-21 is oriented on glass stack lipid samples. The peptide maintained this orientation at different lipid compositions, different peptide concentrations and different temperatures. Preliminary results support a mechanism of toroidal pore formation.

TABLE OF CONTENTS

Dedication……..….ii

Acknowledgements……...iii

Abstract……. iv

Table of contents……v

List of tables……..……...vii

List of figures……..…….viii

Chapter 1: Introduction……..……..1

1.1 Innate immunity…….1

1.2 Antimicrobial peptides……...1

1.3 Cathelicidins……..3

1.4 Mechanism of action of AMP's…….……5

1.5 The only human cathelicidin, LL-37…….7

1.6 Mechanism of lipid bilayer disruption by LL-37…….10

1.7 RK-21 an analog of LL-37……...11

1.8 Antimicrobial properties of RK-21……..12

1.9 Solid phase peptide synthesis……...13

1.10 Nuclear magnetic resonance……15

1.11 Research goal……..…….……....17

Chapter 2: Experimental……..19

2.1 Synthesis of fluorine labeled antimicrobial peptide RK-21…..……..19

2.2 Peptide cleavage……..20

2.3 HPLC purification……...21

2.4 NMR samples……..21

Chapter 3: Results ……..…….…….…….24

3.1 ^{31}P-NMR ……..…….……...24

3.2 ^{19}F-NMR……..……...……..25

Chapter 4: Discussion…….……..34

4.1 DMPC lipid bilayer perturbation by FRK-21….……..……34

4.2 FRK-21 orientation on DMPC…….……..……...35

4.3 FRK-21 acts similarly on different lipid bilayers…….…….....38

Chapter 5: Conclusion……..39

References……40

LIST OF TABLES

1.1 Different classes of antimicrobial peptides with examples……....2

1.2 Categories of cathelicidins with examples…….3

1.3 Various diseases with altered LL-37 concentrations…….….8

1.4 MIC of LL-37 against various microorganisms…….…….9

1.5 MIC of RK-21 against various bacteria…….……13

3.1 ^{19}F-NMR chemical shift values of 2.0m% and 5.0m% FRK-21……26

3.2 ^{19}F-NMR chemical shift values of 2.0m% FRK-21 in DMPC/DMPG…..31

LIST OF FIGURES

1.1 Diagramatic representation of 3 different mechanisms of antimicrobial peptides…..6

1.2 Diagrammatic representation of RK-21 antimicrobial peptide……..12

1.3 Solid phase peptide synthesis…….14

1.4 Anisotropic ^{19}F-NMR resonance frequencies observed on fluoro-phenyl group…..16

2.1 Macroscopic view of lipid glass stack sample……..…….....22

3.1 ^{31}P-NMR spectra of 0.5m% and 2.0m% FRK 21 in DMPC……..…24

3.2 ^{31}P-NMR spectra of 5.0m% of FRK-21 in DMPC……..…..25

3.3 ^{19}F-NMR spectra of 0.5m% FRK-21 in DMPC……26

3.4 ^{19}F-NMR spectra of 2.0m% FRK-21 in DMPC at 15°C…….…..27

3.5 ^{19}F-NMR spectra of 2.0 m% FRK-21 in DMPC at 25°C……27

3.6 ^{19}F-NMR spectra of 2.0m% FRK-21 in DMPC at 35°C……..28

3.7 ^{19}F-NMR spectra of 2.0m% FRK-21 in DMPC at 45°C……..28

3.8 ^{19}F-NMR spectra of 5.0m% FRK-21 in DMPC at 15°C……..29

3.9 ^{19}F-NMR spectra of 5.0m% FRK-21 in DMPC at 25°C……..29

3.10 ^{19}F-NMR spectra of 5.0m% FRK-21 in DMPC at 35°C……..…30

3.11 ^{19}F-NMR spectra of 5.0m% FRK-21 in DMPC at 45°C……..…30

3.12 ^{19}F-NMR spectra of 2.0m% FRK-21 in DMPC/DMPG at 15°C……..…32

3.13 ^{19}F-NMR spectra of 2.0m% FRK-21 in DMPC/DMPG at 25°C……..……32

3.14 ^{19}F-NMR spectra of 2.0m% FRK-21 in DMPC/DMPG at 35°C……..…33

3.15 ^{19}F-NMR spectra of 2.0m% FRK-21 in DMPC/DMPG at 45°C……..…33

4.1 ^{31}P-NMR spectra of various concentrations of FRK-21 in DMPC……...35

4.2 ^{19}F-NMR Temperature series studies of 2.0m% FRK-21 in DMPC samples ……..36

4.3 ^{19}F-NMR Temperature series studies of 5.0m% FRK-21 in DMPC samples……...37

4.4 ^{19}F-NMR spectra of 2.0m% FRK-21 DMPC & DMPC/DMPG (4:1)……..38

CHAPTER 1:

INTRODUCTION

1.1 Innate Immunity

Multi-cellular organisms possess an intrinsic defense mechanism against foreign body infections called innate immunity. Innate immunity is a natural immunity response shown by the organisms when they come into contact with foreign bodies. Innate immunity mainly consists of epithelial barriers, phagocytes, natural killer cells, cytokines and plasma proteins. Antimicrobial peptides are component effector molecules of innate immunity[1].

1.2 Antimicrobial Peptides

Generally antimicrobial peptides are small, have a net positive charge, and are amphipathic in nature[2]. Antimicrobial peptides contain 15 to 45 amino acid residues and are classified into different classes based on their morphological characteristics. Three important classes of scientific interest are linear peptides with α-helical and amphipathic properties, flat dimeric β-sheet peptides with disulfide bonds, and peptides that have certain amino acids in higher levels[2] (e.g. proline, arginine, tryptophan, or histidine). The three classes of antimicrobial peptides with examples are shown in Table 1.1.

Table 1.1. Different classes of antimicrobial peptides with examples.

α-Helical peptides	β-Sheet peptides	Pro/Arg. rich peptides
Human LL-37		
Mice CRAMP	Human α-defensin HNP-1	
Ascaris Cecropin P1		Pig PR-39
Pig VIP(45-72)	Human β-defensin HBD-2	
Frog Maganin 2		Cow Indolicidin
CA(1-7) M(2-9)	Human β-defensin HBD-3	

In mammals, there are two major families of antimicrobial peptides, defensins and cathelicidins, based on their characteristic properties. Defensins are flat molecules, are triple-stranded, and are connected by three intramolecular disulfide bonds. Defensins can be classified into two major groups, α- defensins and β-defensins[3]. These two groups differ in the way the cysteine residues are connected. β-Defensins are generally larger than α-defensins and consist of modified termini. The third group of defensins is called θ-defensins. These are double-stranded, as compared to triple stranded α and β-defensins. Defensins are present in granules of neutrophils of mammals and play an important role in host-defense mechanisms[3].

1.3 Cathelicidins

Cathelicidins are antimicrobial peptides present only in mammals[4]. Though they are structurally diverse, they have a common region similar to cathelin, a 12-kDa protein present in porcine leukocytes[4]. Hence these antimicrobial peptides are named after their common region, cathelin, as cathelicidins. Cathelicidins act against gram-negative bacteria, gram-positive bacteria, fungi, parasites, and enveloped viruses. Along with broad antimicrobial properties, cathelicidins are also involved in activities that indirectly contribute to pathogen removal and help in host defense. These activities include wound repair mechanisms, prevention of tissue injury, promotion of chemotoxic effects at inflammatory sites, and contributions to angiogenesis, antisepsis, and cytotoxicity. Based on morphological characteristics, cathelicidins are broadly classified into four categories that include α-helical, extended helical, loop structure, and β-sheet peptides with 2-3 disulfide bridges[4]. Different categories of cathelicidins with examples are listed in Table 1.2.

Table 1.2. Categories of cathelicidins with examples.

α-Helical	Extended-helical	Loop Structured	β-Sheet
LL-37	Bac4		Protegrin-1
e-CATH-1,2,3	Bac5	Dodecapeptide	Protegrin-2
PMAP-23	Bac7		Protegrin-3
CAP 18	Indolicidin	OaDode	Protegrin-4
P15s	OaBac11		Protegrin-5

α-Helical cathelicidins show a broad spectrum of antimicrobial activity. They have α-helical conformation and are found in humans, monkeys, mice, rabbits, guinea pigs, sheep, cattle, pigs, and horses. These peptides act against gram-positive, gram-negative bacteria and also act effectively against antibiotic-resistant bacteria such as *Staphylococcus aureus, Enterococcus faecalis,* and *Pseudomonas aeruginosa*. In mice, cathelicidins bind to lipopolysaccharide (LPS). LPSs are outer membrane components of gram-negative bacteria and play a major role in initiation of septic shock. Cathelicidins protect mice from LPS lethality by binding to them and neutralizing their activity[4].

Extended-helical cathelicidins are rich in amino acid residues like proline, arginine, or phenylalanine. These antimicrobial peptides are usually present in cattle, sheep, goats, and pigs. These are highly cationic polypeptides and act on enteric gram-negative bacteria[4].

Loop-structured cathelicidins also exhibit potent bactericidal activity against *E. coli* and *S. aureus*. The cyclical cathelicidin dodecapeptide known as bactenecin is a member of this category and contains two cysteine residues[4].

β-Sheet cathelicidins contain 16-18 amino acid residues. The significant characteristic feature of these peptides is the presence of four conserved cysteine residues with intramolecular disulfide bonds and amidated C-terminal arginine residues. These peptides show broad spectrum antimicrobial activity and anti-HIV-1 activity under *in*

vitro conditions. These peptides also display antimicrobicity in physiologic salt conditions and in the presence of serum[4].

1.4 Mechanism of action of AMP's

Antimicrobial peptides bind non-specifically to bacterial cell membranes, due to their net positive charge and the negative charge of the bacterial cell surface (mostly due to negatively charged phosphatidyl esters). Mammalian cell membrane surfaces tend to be more zwitterionic in addition to being stiffened by cholesterol, so they are less attractive to AMPs[2]. AMPs damage the bacterial cell membrane, causing cell lysis and death. An exception is Buforin II, a 21-amino acid antimicrobial peptide, which acts against *Escherichia coli* without damaging the cell membrane but by inhibiting the cellular functions[5]. So far three mechanisms have been proposed to explain the antimicrobial action of these peptides on the bacterial cell membrane. The three mechanisms are barrel-stave pore mechanism, carpet mechanism, and toroidal pore mechanism.

In the barrel-stave mechanism, antimicrobial peptides form pores on the bacterial cell membrane by inserting as oligomers into the membrane. The pores are lined by hydrophilic regions, and their hydrophobic regions face the acyl chains of the bacterial cell membrane lipids. Pore formation leads to cell content leakage and finally cell death. The barrel-stave mechanism is diagrammatically shown in Fig 1.1.

In the carpet mechanism, antimicrobial peptides orient on bacterial cell membranes, disrupting the integrity of the membrane. They act like detergents because they are amphipathic and disrupt the cell membrane by forming micelles around the membrane lipids[6]. The carpet mechanism is shown in Fig 1.1.

In the toroidal pore mechanism, antimicrobial peptides lie on the bacterial cell membrane and induce a curvature strain in the membrane. They form transient, toroidal lipid-peptide pores, leading to content leakage and cell death. The toroidal pore mechanism is shown in Fig 1.1.

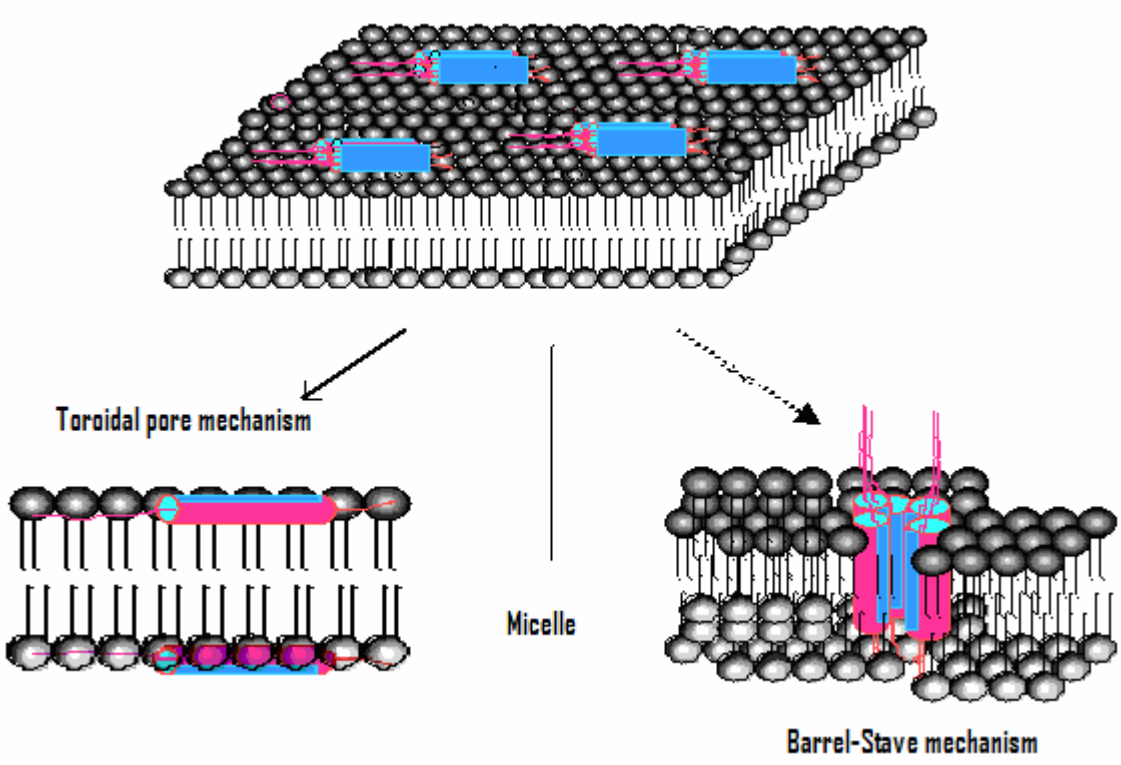

Fig 1.1. Diagrammatic representation of three mechanisms of antimicrobial peptides.

1.5 The only human cathelicidin, LL-37

LL-37 is the only member of cathelicidin group of peptides present in humans. The primary structure of LL-37 is LLGDFFRKSKEKIGKEFKRIVQRIKDFLRNLVPRTES. LL-37 is a 4.5-kDa cationic, amphipathic peptide containing 37 amino acids, of which 16 are charged[7]. Among the 16 charged residues, six Lys and five Arg contribute 11 positive charges, and three Glu and two Asp residues contribute five negative charges, thus resulting in a net positive charge of six at physiological pH. LL-37 also has a total of 14 non-polar amino acids contributing to its amphipathic property. LL-37 forms a α-helical secondary structure under physiological conditions[8].

LL-37 is found in leukocytes, testis, neutrophils, and body fluids and plays a dual role as an antibiotic and signaling molecule. LL-37, acting as a signaling molecule, activates three different receptors: FPRL-1, EGFR, and $P2X_7$. LL-37 concentration is increased or decreased in numerous disease conditions, indicating a correlation with host-defense mechanism. LL-37 plays an important role in antimicrobial activity, cytotoxic activity, lipopolysaccharide binding, chemotactic activity, wound healing, and angiogenesis. The concentration of LL-37 in plasma is around 1.2 mg/L, in normal humans[9]. Several disease states are characterized by irregular levels of LL-37. For example, patients suffering with Morbus Kostmann are devoid of saliva and LL-37. Table 1.3 displays various diseases with altered LL-37 concentrations[8].

Table 1.3. Various diseases with altered LL-37 concentrations[8].

Disease	LL-37 Concentration
Breast cancer	Upregulated
Cystic fibrosis	Upregulated
Cholesteatoma	Upregulated
Psoriasis	Upregulated
Lupus erythematosus	Upregulated
Inflamed synovial membranes	Upregulated
Atopic dermatitis	Downregulated
Chronic ulcer epithelium	Downregulated
Acute myeloid leukemia	Downregulated
Morbus Kostmann	Absent

LL-37 displays a broad spectrum of antimicrobial activities against bacteria, fungi, and viral pathogens. This peptide acts against microbes by non-specifically binding to the outer cell membrane, rupturing the cell membrane and leading to cell death. Table1.4 displays minimum inhibitory concentrations (MIC) of LL-37 against various bacteria and microorganisms.

Table 1.4. MIC of LL-37 against various microorganisms[8].

Organism	LL-37 activity (MIC)
Streptococcus Group A	1-16μM
Streptococcus Group B	≥32μM
Streptococcus Group C	16μM
Staphylococcus aureus	>32μM
Bacillus subtilis	2.7μg/ml
Lactobacillus acidophilus	19μM
Escherichia coli	>32μM
Pseudomonas aeruginosa	16μg/ml
Salmonella typhimurium	3.5μg/ml
Klebsiella pneumoniae	4.2μg/ml
Proteus mirabilis	5.7μg/ml
Capnocytophaga gingivalis	9μg/ml
Treponema pallidum	450μg/ml
Leptospira interrogans	144-225μg/ml
Candida albicans	>20μg/ml

The outer membrane of gram-negative bacteria is made of lipopolysaccharides. During sepsis, bacteria release lipopolysaccharides, called endotoxins. LL-37 strongly binds to lipopolysaccharides, thereby neutralizing their biological toxicity. LL-37 is most effective in the treatment of lethal sepsis in rats[10].

LL-37 shows chemotactic activity in host defense mechanisms. LL-37 attracts T-cell leukocytes, mononuclear cells, and neutrophils. It also stimulates mast cells, thereby causing them to degranulate and release pro-inflammatory mediators, such as histamine and prostagladins, resulting in vascular permeabilization. LL-37 activates three different receptors, FPRL-1, EGFR, and $P2X_7$, which leads to immunostimulatory effects.

LL-37 has been found in higher than normal levels at wound sites and returns to normal levels after the wound heals. In one study, inhibition of LL-37 by specific antibodies prevented wounds from healing[8]. In the epithelium of patients with chronic ulcers, reduced levels of LL-37 were found, indicating a major role played by LL-37 in wound healing.

1.6 Mechanism of lipid bilayer disruption by LL-37

Like all antimicrobial peptides, three basic mechanisms have been proposed for the membrane disrupting activity of LL-37: barrel-stave, detergent, and toroidal pore mechanisms. In a research study on LL-37, using polarized attenuated total reflectance Fourier transform infrared spectroscopy, it was found that LL-37 predominantly existed as α-helical and was oriented parallel to the surface of zwitterionic lipid membranes, showing no sign of barrel-stave pores[11]. Henzler-Wildman et al. investigated the effect of LL-37 on different lipid bilayer compositions at various peptide concentrations and temperatures. ^{15}N-NMR studies of labeled LL-37 showed that LL-37 orients parallel to the lipid bilayer surface. LL-37 maintained the orientation at different compositions of lipid bilayers, at various peptide concentrations, and in temperature studies. This

indicated that LL-37 does not act by the barrel-stave model[12]. ^{31}P-NMR experiments on oriented lipid bilayers with LL-37 did not show any isotopic peaks characteristic of micelles or small membrane fragments. This ruled out the detergent-like action by LL-37. In ^{31}P spectra and calorimetric studies done by Henzler-Wildman, LL-37 induced positive curvature strain in the lipid bilayer. The small size of lipid head groups compared to long acyl chains results in a negatively curved phase in lipid bilayer. When LL-37 is added to the lipid bilayer, it inhibits the negative curvature. These results confirm that LL-37 induces positive curvature strain in the bilayer. The induction of positive curvature strain was seen in different lipid and peptide environments. These experimental results confirmed that LL-37 most likely acts against bacteria by a toroidal-pore mechanism[6].

1.7 RK-21 an analog of LL-37

RK-21 is a fragment of LL-37. The RK-21 primary structure is RKSKEKIGKEFKRIVQRIKDF. RK-21 constitutes most of the helical region of LL-37, forming its core portion as shown in the Fig 1.2. RK-21 consists of 21 amino acid residues, of which nine are positively charged and three are negatively charged at physiological pH. Out of the nine positively charged amino acid residues, six are lysine residues and three are arginine residues. Two glutamic acid residues and one aspartic acid residue contribute negative charges at physiological pH. The net charge on RK-21 at physiological pH therefore is +6, the same as parent LL-37.

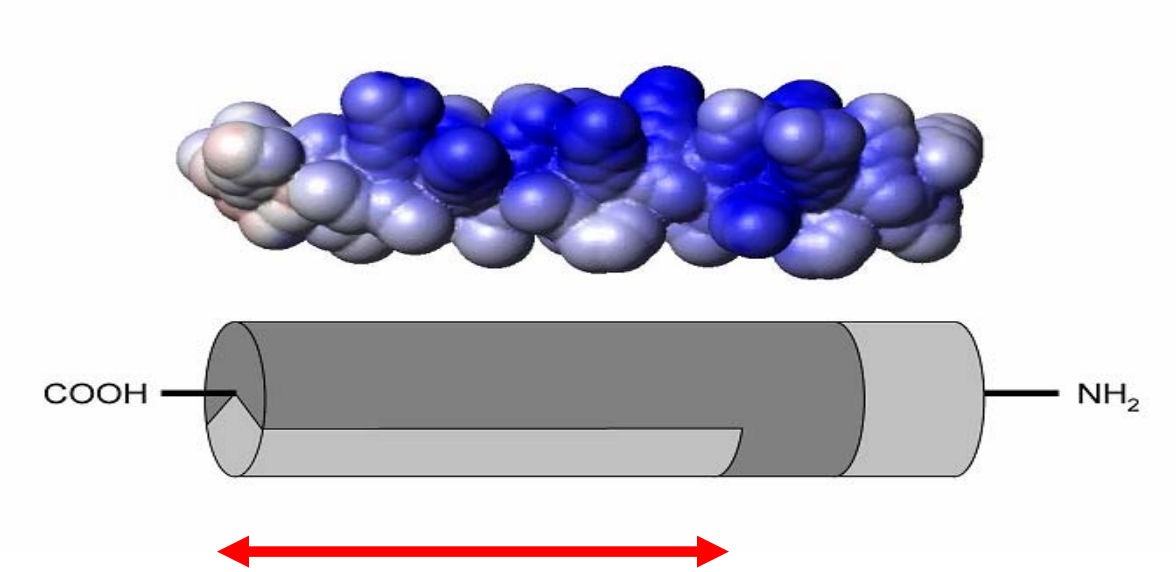

Fig 1.2. Diagrammatic representation of RK-21 antimicrobial peptide.

1.8 Antimicrobial properties of RK-21

RK-21 showed antimicrobial activity against various gram-positive and gram-negative bacteria and was effective against *Escherichia coli* at a low 0.4µg/ml concentration[13]. Table1.5. gives a detailed listing of RK-21 antimicrobicity against various bacteria. These are comparable to values obtained for LL-37 at zero millimolar NaCl concentration.

Table 1.5. MIC of RK-21 against various bacteria.

Bacterial Strain	**LL21 Activity (μg/ml)**[13]	**LL37 Activity (μg/ml)** [14]
Porphyromonas gingivalis W83	12.5	< 10
Staphylococcus aureus	50	2.9
Salmonella enterica	50	< 10
Pseudomonas aeruginosa	100	12
S. gordonia	6.25	< 10
Enterococcus feacalis FA2-2	12.5	3.5
Enterococcus feacalis OG1X	50	3.5
Escherichia coli	0.4	0.1
Bacillus subtilis	Enhancer (0.1)	2.7

1.9 Solid Phase Peptide Synthesis

In solid phase peptide synthesis, a polystyrene resin forms a strong solid support for building the amino acid chain. Initially the carboxyl group of an N-protected amino acid reacts with a hydroxyl or amide group of the resin and forms a covalent bond, with loss of a water molecule. In the next step, a deprotection is carried out and now the reactive amino group of the attached amino acid is free to react with the carboxyl group of the next incoming N-protected amino acid (which forms an activated ester due to an activating agent), forming a peptide bond. These steps–deprotection, washes, and coupling–are repeated until the end of peptide sequence. After the completion of peptide

synthesis, the peptide chain is cleaved from the resin. This cleavage also removes side chain protecting groups that are still intact. Figure 1.3. diagrammatically represents solid phase peptide synthesis[15].

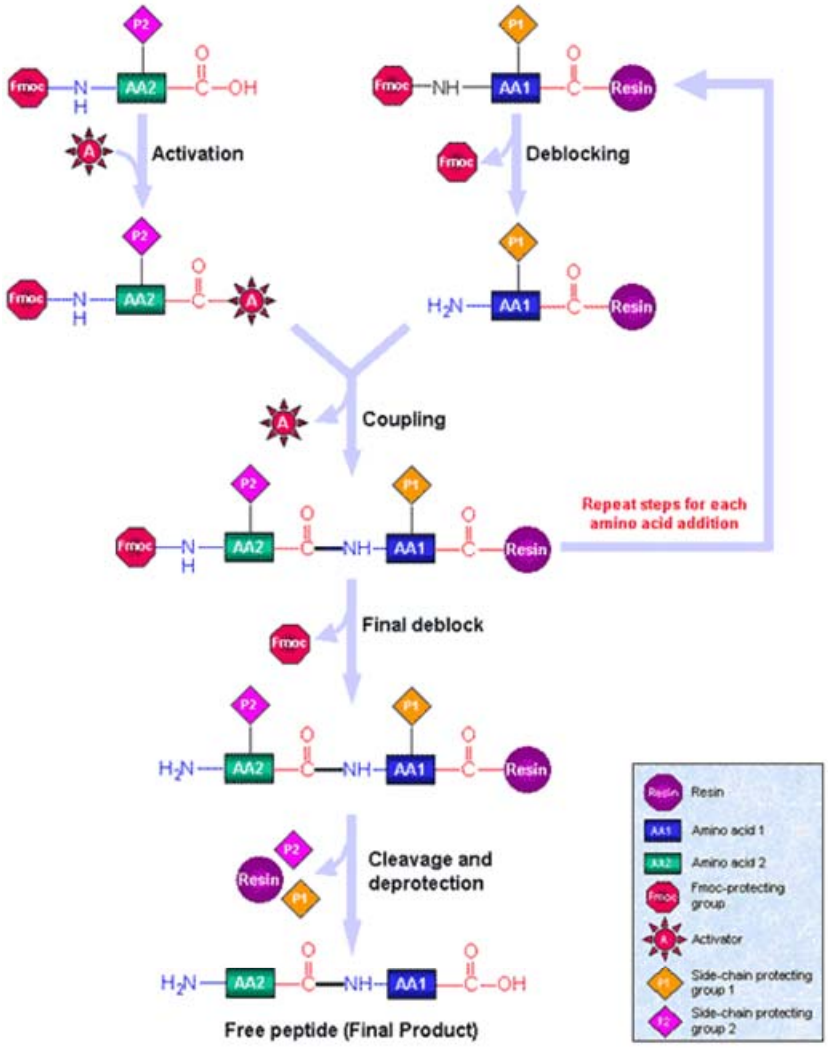

Fig 1.3. Solid phase peptide synthesis.

RK-21 was synthesized using N-α-fluorenylmethyloxycarbonyl (Fmoc) protected amino acids and p-methylbenzhydrylamine resin (MBHA). Piperidine (20%) in N, N-dimethylformamide (DMF) was used for deprotection. O-(Benzotriazol-l-yl)-1, 1, 3, 3-tetramethyluronium hexafluorophosphate (HBTU) was used as a coupling agent.

1.10 Nuclear magnetic resonance

Most elementary particles like atomic nuclei have nuclear spin. Nuclear spin is a form of angular momentum, represented by $\vec{I}$. Nuclear spin is related to magnetic moment (μ) and is proportional to nuclear spin angular momentum: $\mu = \gamma \vec{I}$. Gyromagnetic ratio represented by γ is the fundamental property of each nucleus.

When a nucleus with a spin is placed in a strong magnetic field, then there is splitting of energy levels. This splitting of energy levels allows the nucleus to make transitions between different energy spin states. These transitions can be achieved by absorption or emission of radiation in the radiofrequency wavelength range.

The effective field strength acting on a specific nucleus depends on the local electronic environment of that nucleus. The surrounding environment causes a shift in the resonance frequency called a chemical shift. Whenever the molecule under study is motionally restricted, then chemical shift anisotropy (CSA) is seen in the NMR spectra. These spectral effects are very small and are therefore represented as parts per million (ppm). So, the shielding effected by the electron cloud surrounding a nucleus will be different for different orientations of the molecule with respect to the external magnetic

field. Anisotropic effects are not prominent in liquid samples as these effects are hidden by constant thermal motion of liquid molecules. Thus in motionally restricted samples, the chemical shift anisotropy can be exploited to attain its orientation.

In crystalline samples, powder samples, and liquid samples, all possible molecular orientations are present. These samples yield very broad NMR line shapes. These broad lines possess characteristic shapes, called “powder pattern” or “tensor line shapes.”

The highly anisotropic geometry of the phenyl π-electron ring of *p*-F-phenylalanine yields significant effects. When the phenyl ring plane is perpendicular to the external magnetic field, the π-electrons will effectively shield the fluorine nucleus, yielding a low value of chemical shift around -155 ppm as shown in Fig 1.4.

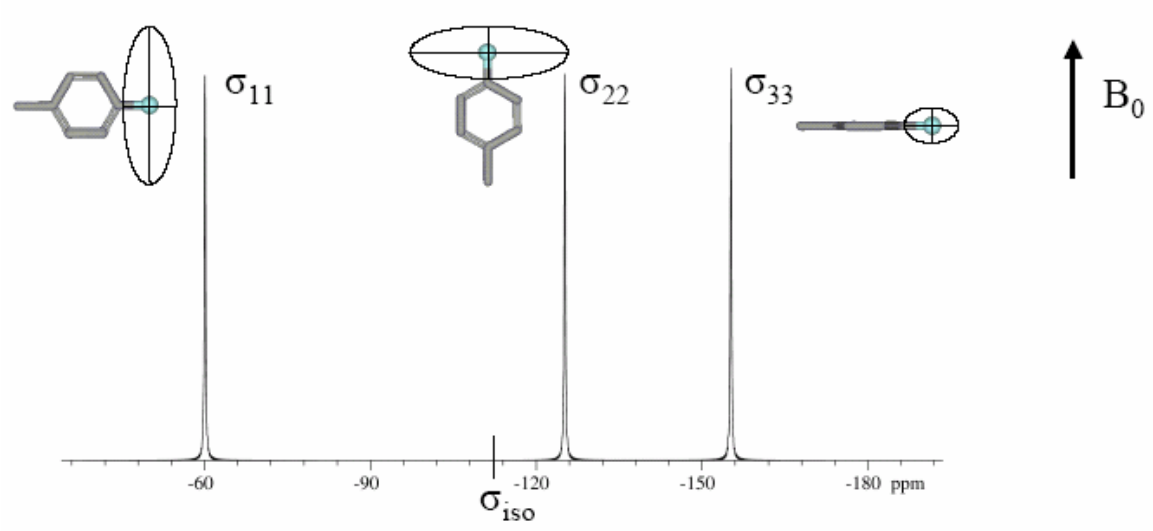

Fig 1.4. Anisotropic ^{19}F-NMR resonance frequencies observed on fluoro-phenyl group[16].

When the phenyl ring plane is oriented normal and the long axis is perpendicular to the external magnetic field, then shielding is ineffective and yields a high chemical shift around -60 ppm, as shown in Fig 1.4.

The other possible orientation is the C-F connecting bond lining up with the magnetic field, which results in intermediate shielding with a chemical shift around -125 ppm, as shown in Fig 1.4.

1.11 Research Goal

RK-21 showed similar antimicrobial properties to its parent LL-37. The other advantages of RK-21 are its ease for chemical synthesis due to its short sequence, and its lower economic cost. The goal of the research project was to synthesize isotopically labeled RK-21 and study its orientation on the lipid bilayer using ^{19}F-NMR. In order to study the disruption of lipid bilayer, ^{31}P-NMR experiments were performed. The aims of the research project were

1. To replace the 11th position phenylalanine with 4-^{19}Fluoro phenylalanine and synthesize the fluorine labeled RK-21 with the double coupling method.
2. To perform ^{31}P-NMR studies on lipid bilayers with labeled peptide RK-21.
3. To perform ^{19}F-NMR studies on fluorine labeled RK-21.
4. To perform ^{19}F-NMR studies at various peptide concentrations: 0.5 mol%, 2.0mol%, and 5.0mol% of labeled RK-21 peptide concentration.

5. To perform NMR studies on different lipid composition bilayers: DMPC and DMPC/DMPG (4:1) lipid bilayers.
6. To perform temperature series studies on labeled RK-21.

The main research goal was to understand the mechanism of lipid bilayer disruption by RK-21.

CHAPTER 2:

EXPERIMENTAL

2.1 Synthesis of fluorine-labeled antimicrobial peptide RK-21

Fluorine-labeled RK-21 (FRK-21) was synthesized by replacing the phenylalanine at the 11^{th} position of RK-21 with fluorine labeled 4-^{19}F-phenylalnine. All amino acids used were protected by the N-α-fluorenylmethyloxycarbonyl (Fmoc) group. The resin used in the solid phase peptide synthesis was Rink amide methylbenzhydrylamine (MBHA) resin. O-(Benzotriazoylyl)-1, 1, 3, 3 - tetramethyluroniumhexafluorophosphate (HBTU) was used as coupling agent in peptide synthesis. 0.4 M N, N- diisopropylethylamine in dimethylformamide (DMF) was used as the activator in peptide synthesis, and 20% v/v piperidine in DMF was the deprotectant solution. DMF was also utilized for washing steps. All FMOC-protected amino acid residues of F-RK21 were weighed equivalent to their 0.4 mmoles. For example, the molecular weight of protected arginine is 662.8g/mole, so 0.4 millimoles of this would be 0.4 mmoles x 662.8 g/mol /1000 = 0.2651g. Along with the amino acid residue, 0.4 millimoles of HBTU (0.152g) was also weighed and added to each vial of amino acid. Amino acids were weighed in duplicate, in order to synthesize the peptide by the double coupling technique, to improve the yield. This means that after the first vial of amino acid reacts for an hour, the contents of the vessel are cleared and the second vial is added to couple with any unreacted sites. All of the amino acid vials were placed on the automated PS3 peptide synthesizer, according to the desired sequence, and peptide synthesis was

carried out automatically on the PS3 peptide synthesizer with repetitive deprotection, washing, and coupling steps.

2.2 Peptide Cleavage

After the completion of the entire sequence, the vessel containing FRK-21 with resin was removed from the automated PS3 peptide synthesizer. The FRK-21-resin was washed with DMF and methylene chloride. The peptide-resin was dried under vacuum for one hour. A fresh cleavage solution was prepared by adding 0.5 ml of anisole, 0.5 ml of distilled water, 0.5 ml of thioanisole, one crystal of phenol, and 10.0 ml of trifluoroacetic acid. The cleavage solution was added to the mixture under controlled temperature, at 0 °C, in an ice bath. The mixture was then stirred for three hours at room temperature. The mixture was filtered, to remove the uncharged resin. The cleaved, dissolved FRK-21 was precipitated by adding 50 ml cold diethyl ether and recovered by filtration. The precipitated peptide was dissolved in 70% acetonitrile/H_2O, and an equal amount of distilled water was added to it. The peptide solution was frozen at -70 °C and lyophilized overnight.

2.3 **HPLC purification**

A Waters HPLC (501 and 510 pumps) with Waters 484 detector was used. A Phenomenex Jupiter C18 column, 250mm x 21.2mm, 10μ, was used to purify the FRK-21 peptide. A gradient separation, with increasing organic composition (10 to 50% over 2 hrs), was programmed to purify the peptide. Mobile phase A was made of 0.1% HCl-water, and mobile phase B was made of 0.1% HCl-acteonitrile. The lyophilized FRK-21 was dissolved in acetonitrile and injected into the reverse phase HPLC. The detector was set at 254nm, to record the chromatogram. The purified peptide was collected in test tubes, which were combined and lyophilized overnight. The purity of FRK- 21 was tested by analytical RP-HPLC, using a Phenomenex Jupiter 5μ, C18, 250 x 4.6mm column, using a gradient program of 0 to 66% organic component over 33 min with the same mobile phase composition. The molecular weight of the peptide was confirmed by MALDI-TOF mass spectrometry. The molecular weight was 2650.4, and the purity as analyzed by HPLC peak integration was more than 96%. A yield of 59.7mg of FRK-21 was obtained.

2.4 **NMR samples**

Two different lipid bilayer systems were used: dimyristylphosphotidylcholine (DMPC) and DMPC: dimyristylphosphotidylglycerol (DMPC/DMPG) in a ratio of 4:1. The peptides and lipids were mixed in chloroform: methanol (2:1) solution. The mixture was dried under nitrogen and resuspended in chloroform:methanol (2:1) solution. The solution was spread on a thin glass plate and air dried. In a similar way, a stack of 17 glass plates, one above the other with a middle lipid protein layer, was prepared. The

stack was vacuum dried overnight. Finally, the plates were indirectly hydrated in a hydration chamber. The lipid bilayer orients by mimicking the bacterial cell membrane between the glass plates, with oriented peptides as shown in Fig 2.1.

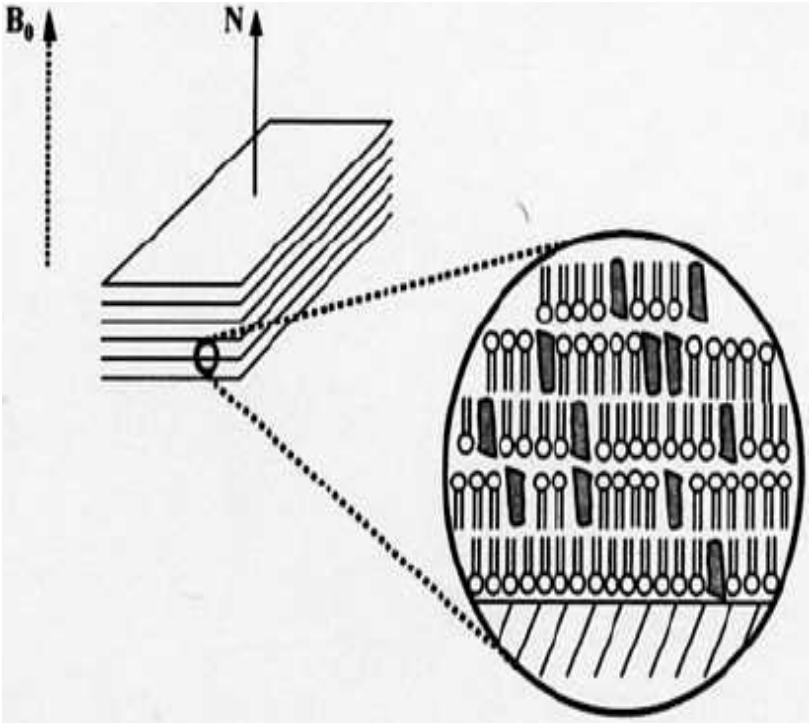

Fig 2.1. Macroscopic view of lipid glass stack sample[15].

In a similar way, FRK-21 peptide samples of 0.5 mol% (moles of peptide relative to total moles of lipid+peptide), 2.0mol%, and 5.0mol% in DMPC-glass plates were prepared. FRK-21 peptide sample of 2.0mol% in DMPC/DMPG (4:1) glass plates was prepared in a similar manner. The NMR spectra were acquired on these samples at 500 MHz frequency.

CHAPTER 3:

RESULTS

3.1 ^{31}P-NMR

The effect of FRK-21 on the lipid bilayer (DMPC) was studied using ^{31}P solid state NMR on 0.5m%, 2.0m%, and 5.0m% peptide /DMPC samples. The ^{31}P-NMR spectra of 0.5m% FRK-21 in DMPC and 2.0m% FRK 21 in DMPC each showed a single peak, as shown in Fig 3.1.

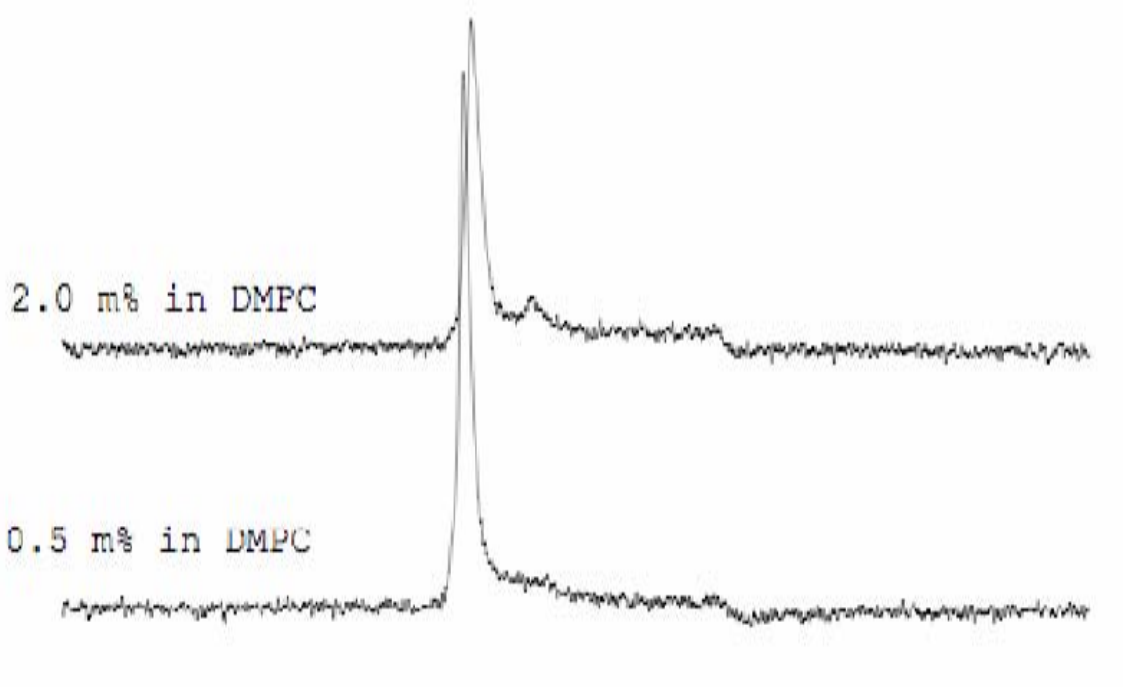

Fig 3.1. ^{31}P-NMR spectra of 0.5m% and 2.0m% FRK 21 in DMPC.

The ^{31}P-NMR spectra of 5.0% FRK-21 in DMPC showed a single broader peak, as shown in Fig 3.2.

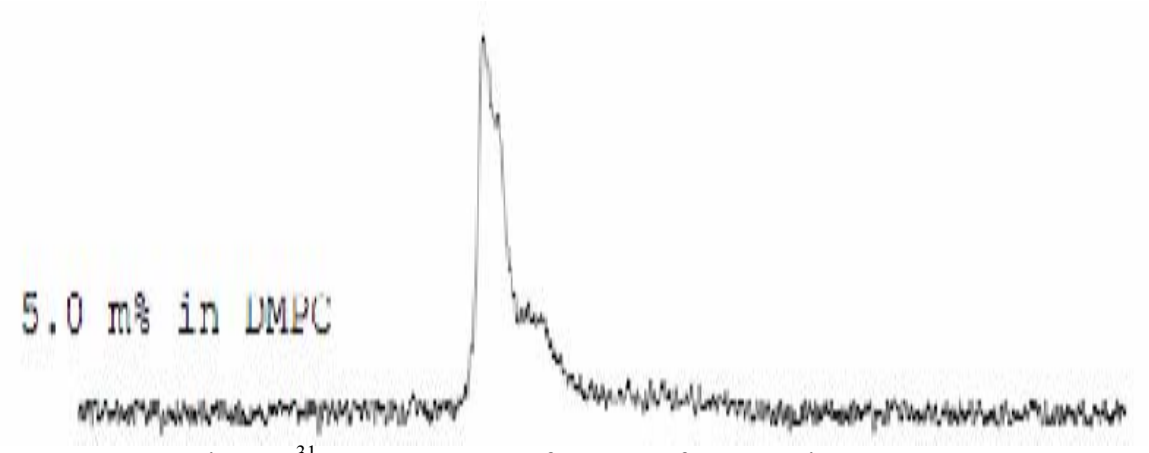

Fig 3.2. ^{31}P-NMR spectra of 5.0m% of FRK-21 in DMPC.

With the increasing concentration of FRK-21 in DMPC glass stack samples, the peak broadened. There was no micelle-characteristic peak seen in the ^{31}P-NMR studies.

3.2 ^{19}F-NMR

In order to understand the orientation of FRK-21 on the lipid bilayer (DMPC), ^{19}F-solid state NMR studies were done. ^{19}F-NMR studies were performed on 0.5m%, 2.0m%, and 5.0m% FRK-21 in DMPC glass plate samples. Temperature series experiments were done at 15°C, 25°C, 35°C, and 45°C on 2.0m% and 5.0m% FRK-21 in DMPC glass stack samples.

The ^{19}F-NMR spectra of 0.5m% FRK-21 in the DMPC lipid glass stack sample showed a peak at a chemical shift value of -110.4ppm, as shown in Fig 3.3.

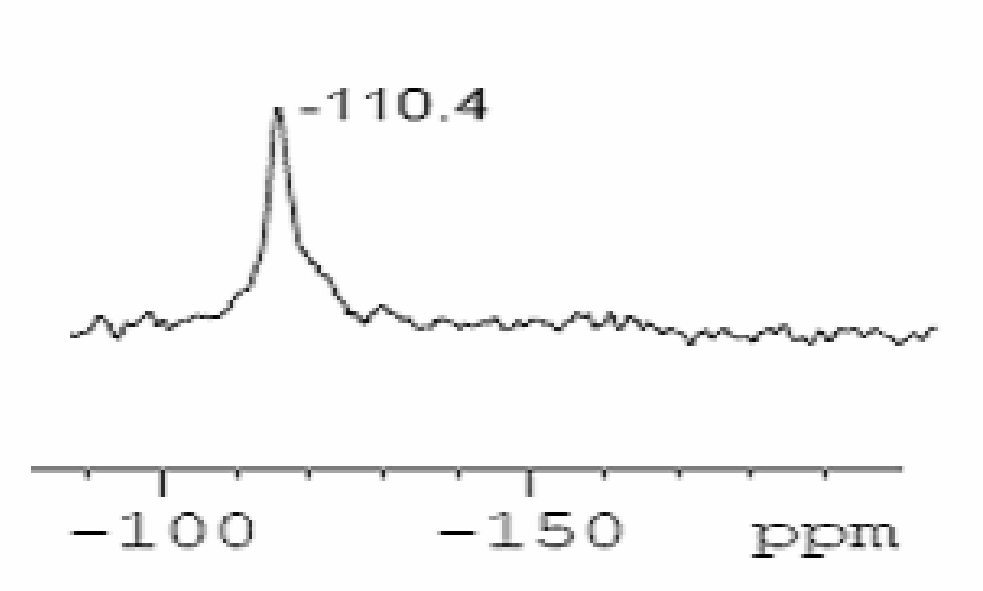

Fig 3.3. ^{19}F-NMR spectra of 0.5m% FRK-21 in DMPC.

The ^{19}F-NMR chemical shift values of 2.0m% and 5.0m% FRK-21 in DMPC lipid glass stack samples at 15°C, 25°C, 35°C and 45°C are shown in Table 3.1.

Table 3.1. ^{19}F-NMR chemical shift values of 2.0m% and 5.0m% FRK-21.

Temperature (°C)	2.0 m% FRK-21 δ (ppm)	5.0 m% FRK-21 δ (ppm)
15	-114.0	-114.5
25	-112.2	-114.6
35	-111.3	-114.8
45	-112.3	-111.6/-114.9

The ^{19}F-NMR spectra of 2.0m% FRK-21 in DMPC lipid glass stack samples at 15°C, 25°C, 35°C, and 45°C are shown from Fig 3.4 to Fig 3.7.

Fig 3.4. ^{19}F-NMR spectra of 2.0m% FRK-21 in DMPC at 15°C.

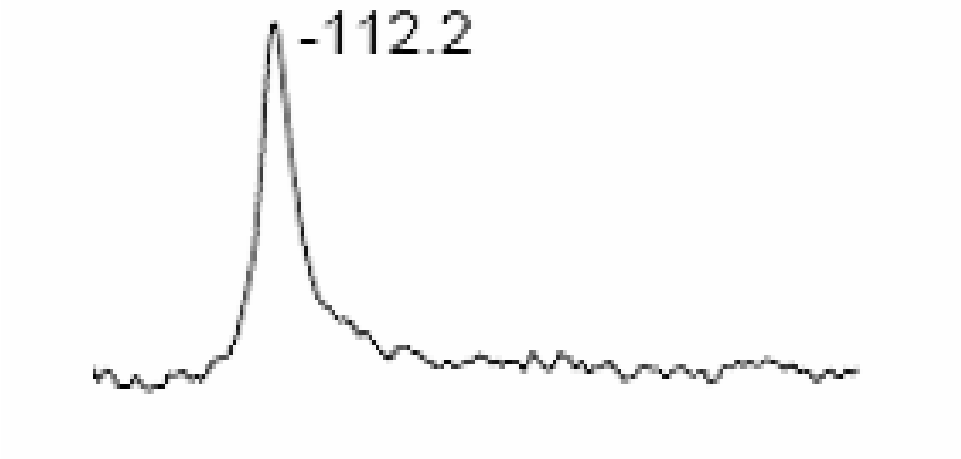

Fig 3.5. ^{19}F-NMR spectra of 2.0 m% FRK-21 in DMPC at 25°C.

.

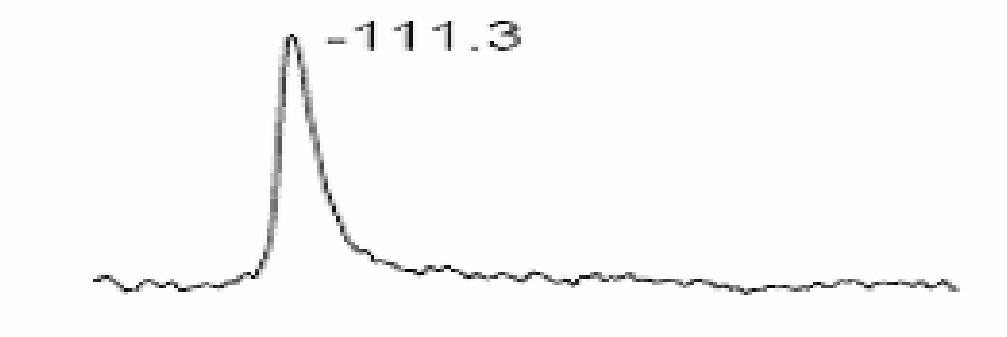

Fig 3.6. ^{19}F-NMR spectra of 2.0m% FRK-21 in DMPC at 35°C.

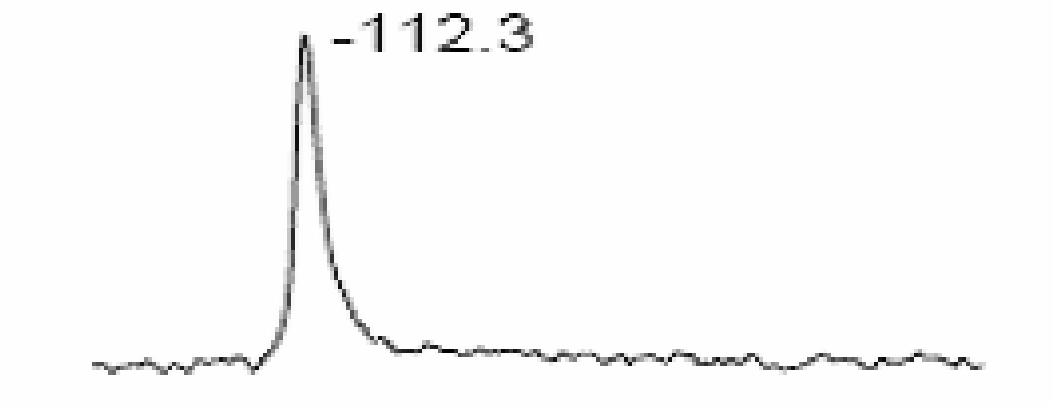

Fig 3.7. ^{19}F-NMR spectra of 2.0m% FRK-21 in DMPC at 45°C.

The ^{19}F-NMR spectra of 5.0m% FRK-21 in DMPC lipid glass stack samples at 15°C, 25°C, 35°C, and 45°C are shown from Fig 3.8 to Fig 3.11.

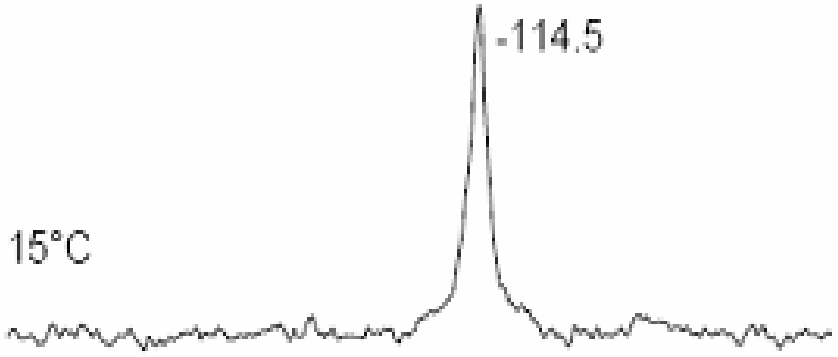

Fig 3.8. ^{19}F-NMR spectra of 5.0m% FRK-21 in DMPC at 15°C.

.

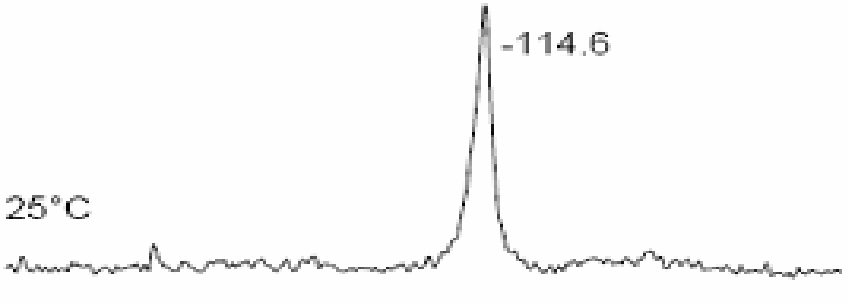

Fig 3.9. ^{19}F-NMR spectra of 5.0m% FRK-21 in DMPC at 25°C.

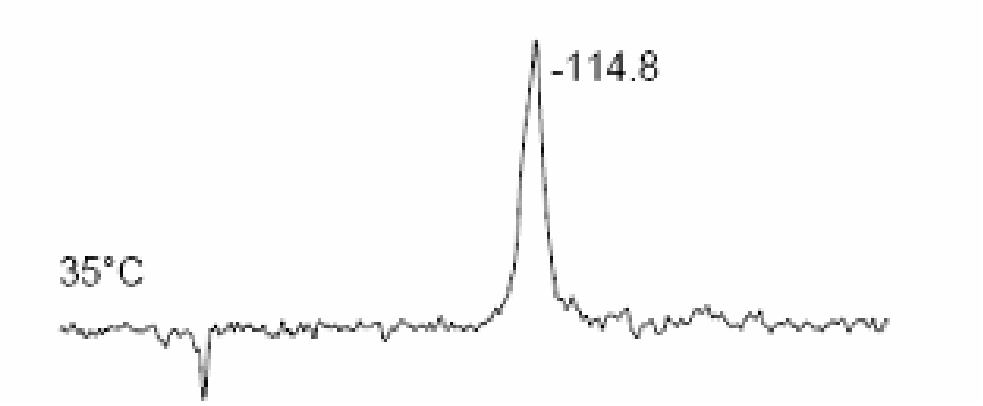

Fig 3.10. ^{19}F-NMR spectra of 5.0m% FRK-21 in DMPC at 35°C.

Interestingly, the ^{19}F-NMR spectra of 5.0m% FRK-21 in a DMPC lipid glass stack sample showed a peak at a chemical shift value of -114.9ppm and a second spectral component at -111.6 ppm at 45°C, as shown in Fig 3.11.

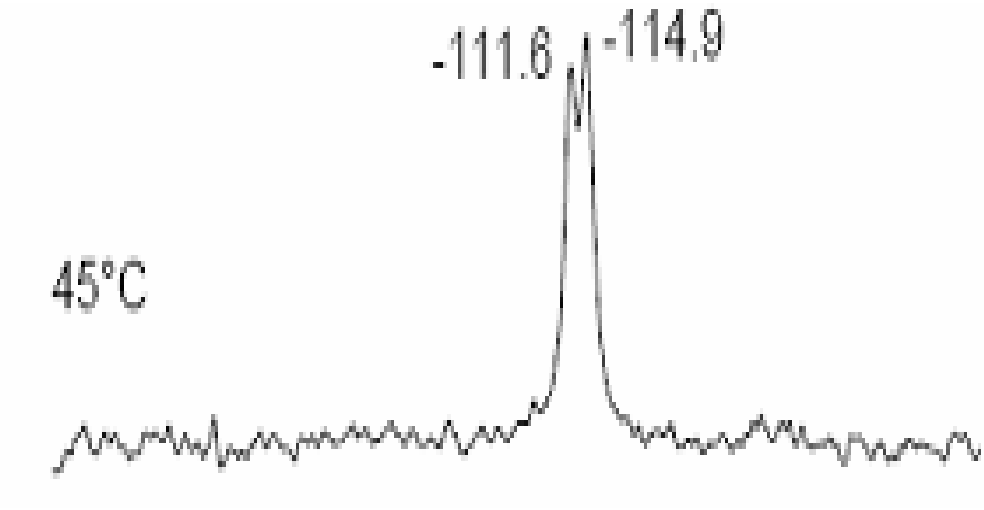

Fig 3.11 ^{19}F-NMR spectra of 5.0m% FRK-21 in DMPC at 45°C.

Overall, the CSA values shifted slightly with increasing concentration of FRK-21 in DMPC lipid bilayer samples. In the ^{19}F-NMR spectra of 5.0m% FRK-21, the additional spectral component at -111.6ppm has the same chemical shift value as those of the lower peptide FRK-21 concentration.

In order to study the orientation and behavior of FRK-21 in a different lipid bilayer system, ^{19}F-NMR studies were done on samples containing DMPC/DMPG (4:1) lipid bilayers with FRK-21. ^{19}F –NMR studies were performed on samples with 2.0m% of FRK-21 in a DMPC/DMPG (4:1) glass stack sample. These samples were analyzed at temperatures of 15°C, 25°C, 35°C, and 45°C.

The ^{19}F-NMR chemical shift values of 2.0m% FRK-21 in DMPC/DMPG (4:1) glass stack sample at 15°C, 25°C, 35°C, and 45°C are shown in Table 3.2.

Table 3.2. ^{19}F-NMR chemical shift values of 2.0m% FRK-21 in DMPC/DMPG (4:1).

Temperature (°C)	δ (ppm)
15	-113.2
25	-111.9
35	-112.1
45	-112.1

The ^{19}F-NMR spectra of 2.0m% FRK-21 in a DMPC/DMPG (4:1) glass stack sample at 15°C, 25°C, 35°C, and 45°C are shown from Fig 3.12 to Fig 3.15, respectively.

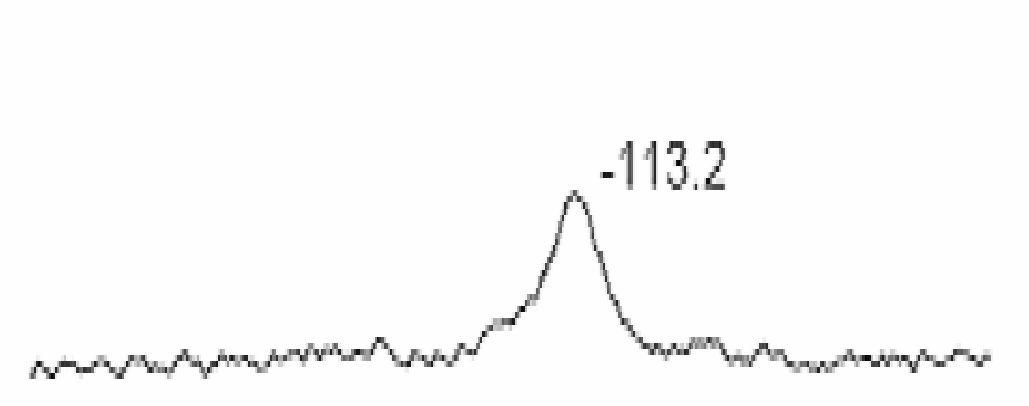

Fig 3.12. ^{19}F-NMR spectra of 2.0m% FRK-21 in DMPC/DMPG at 15°C.

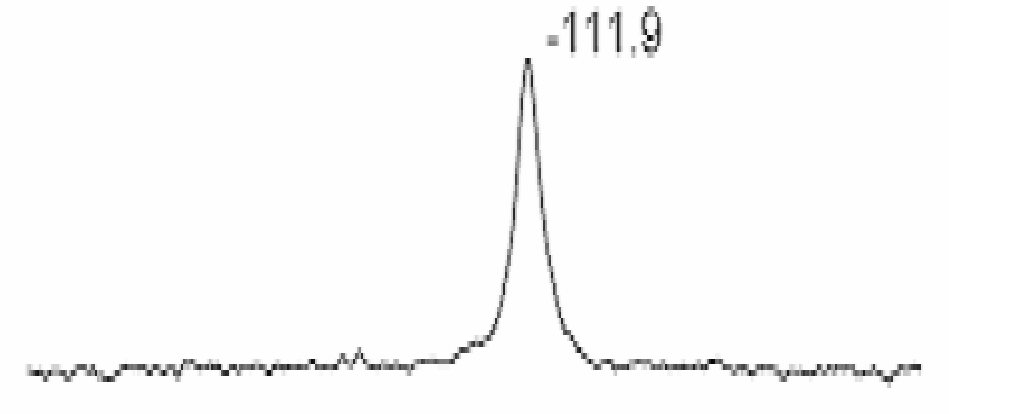

Fig 3.13. ^{19}F-NMR spectra of 2.0m% FRK-21 in DMPC/DMPG at 25°C.

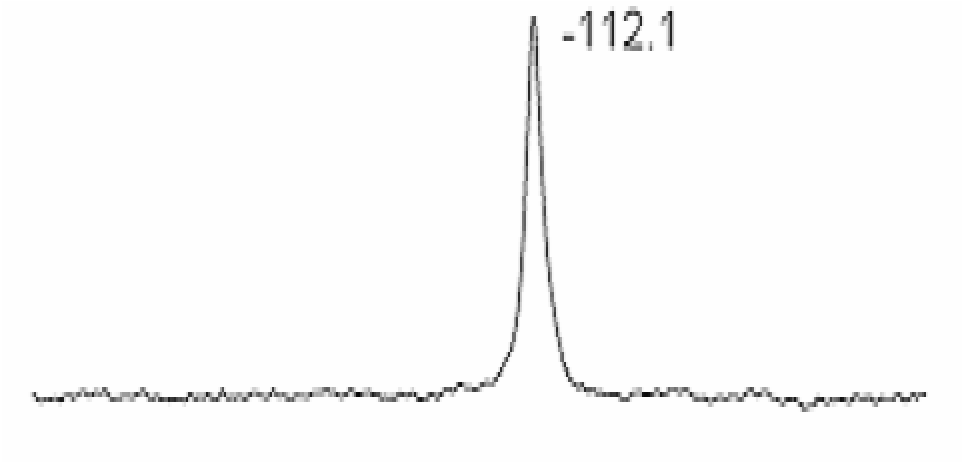

Fig 3.14. ^{19}F-NMR spectra of 2.0m% FRK-21 in DMPC/DMPG at 35°C.

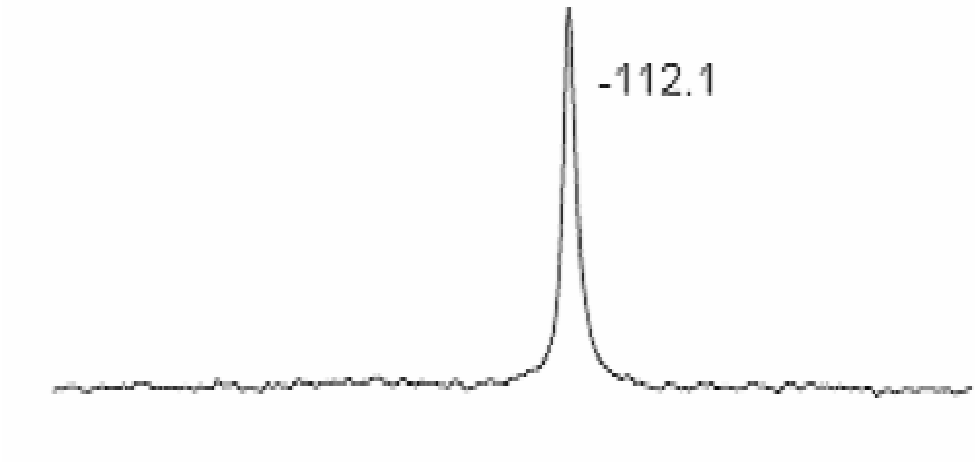

Fig 3.15. ^{19}F-NMR spectra of 2.0m% FRK-21 in DMPC/DMPG at 45°C.

CHAPTER 4:

DISCUSSION

4.1 DMPC lipid bilayer perturbation by FRK-21

The ^{31}P-NMR spectra of 0.5m% FRK-21 in DMPC glass stack samples showed a narrow peak. The 2.0m% FRK-21 incorporated into the DMPC bilayer showed the same oriented peak as the 0.5m% sample but was slightly broader, indicating that FRK-21 at higher concentration (2.0m%) induces a conformational change in the lipid head groups. The peak broadened further in the 5.0m% FRK-21 sample, confirming that at higher concentrations the FRK-21 perturbs the DMPC lipid bilayers. However, the ^{31}P-NMR studies did not yield any peak characteristic of micelle or small lipid fragments as shown in Fig 4.1. These results suggest that 1) the peptide is oriented on the DMPC lipid glass stack samples; 2) the peptide induces conformational changes in the lipid head groups, perturbing the lipid bilayer; and 3) the FRK-21 does not act by a detergent-like mechanism, as indicated by the absence of micelle-characteristic peaks. In the detergent-like or carpet mechanism, pieces of the membrane are fragmented, which would result in additional micellar peaks in the spectra.

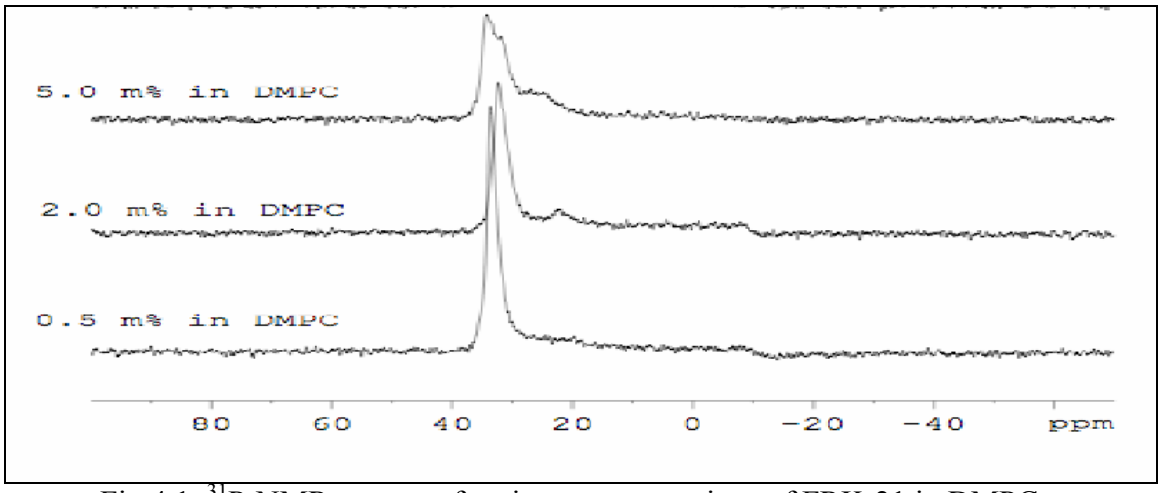

Fig 4.1. ^{31}P-NMR spectra of various concentrations of FRK-21 in DMPC.

4.2 FRK-21 orientation on DMPC

The ^{19}F-NMR spectra on 2.0m% and 5.0m% FRK-21 in DMPC lipid samples show a similar pattern. At all concentrations and temperatures tested, the FRK-21 maintained its orientation, as shown in Fig 4.2 and Fig 4.3. There is only a slight change in chemical shift values with increasing FRK-21 concentrations. Since the peptide did not change its orientation with increasing concentration, this indicates that it does not form barrel-stave pores and excludes the barrel-stave mechanism. In this mechanism, the peptide first orients parallel to the membrane surface and then inserts into the membrane perpendicular to the surface. The evidence indicates that this did not occur. The ^{19}F-NMR spectra of 5.0m% FRK-21 in a DMPC glass stack sample at 45°C showed a second spectral component with a chemical shift value of -111.6 ppm. This is close to the chemical shift value observed at lower FRK-21 concentration (-111.3 at 2.0m% FRK-21, -110.4 ppm at 0.5m% FRK-21). This indicates the possible formation of a dimer of FRK-21 at higher concentration (5.0m %).

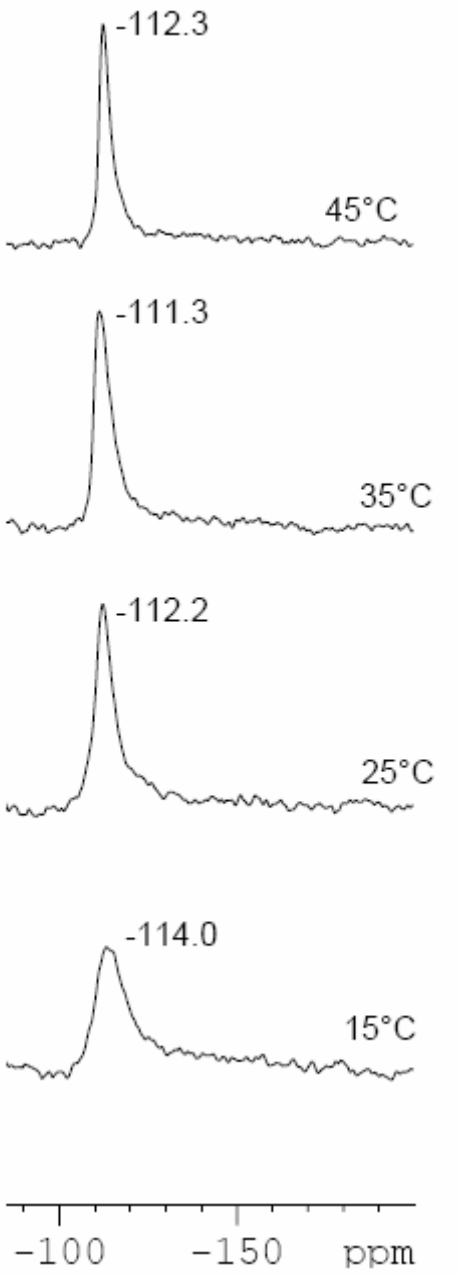

Fig 4.2. ^{19}F-NMR Temperature series studies of 2.0m% FRK-21 in DMPC samples.

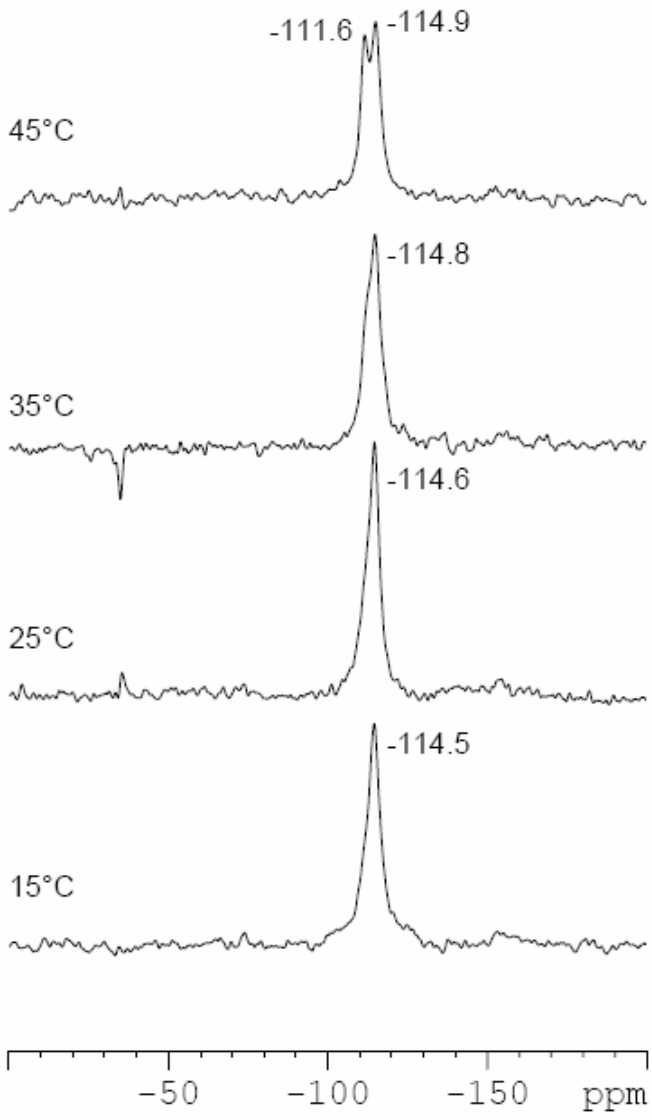

Fig 4.3. ^{19}F-NMR Temperature series studies of 5.0m% FRK-21 in DMPC samples.

4.3 FRK-21 acts similarly on different lipid bilayers

^{19}F-NMR spectra of 2.0m% FRK-21 in two different lipid bilayers, DMPC and DMPC/DMPG (4:1) at different temperatures, showed very similar chemical shift values, as shown in Fig 4.4. This indicates that FRK-21 oriented in a similar way in these different lipid bilayers.

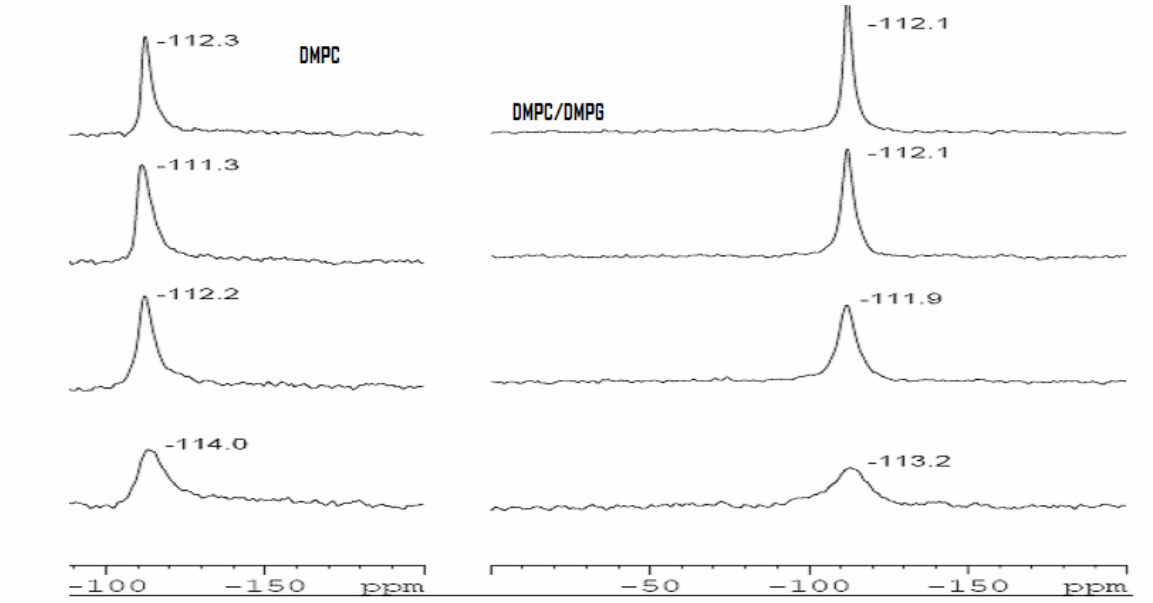

Fig 4.4. ^{19}F-NMR spectra of 2.0m% FRK-21 DMPC & DMPC/DMPG (4:1).

CHAPTER 5:

CONCLUSION

Based on ^{31}P-NMR studies, which did not show any micellar or membrane fragments, we can eliminate the detergent-like mechanism for FRK-21. ^{19}F-NMR studies indicated that fluorine labeled RK-21 is oriented on glass stack lipid samples. The peptide maintained this orientation at different lipid compositions, at different peptide concentrations, and at different temperatures, thus ruling out the barrel stave mechanism. Therefore, preliminary results support a mechanism of toroidal pore formation.

References:

1. Abbas, K. A., Andrew, H.L. *Basic Immunology functions and disorders of the immune system,* Jason, M. 2nd edition, Elsevier, Philadelphia, PA, 2004, pp 21-38.
2. Boman, H.G. *J.Inter.Med*. **2003**, *254*, 197-215.
3. Hosokawa, I.; Hosokawa, Y.; Komatsuzawa, H.; Goncalves, R.B.; Karimbux, N.; Napimoga, M.H.; Seki, M.; Ouhara, K.; Sugai, M.; Taubman, M.A.; Kawai, T. *Clin. Exp. Immunol.* **2006**. *146* 218-225.
4. Ramanathan, B.; Davis, E.G.; Ross, R.C.; Blecha, F. *Microbes and Infection*. **2002**, 4, 361-372.
5. Park, C.B.; Kim, H.S.; Kim, S.C. *Biochem. Biophys. Res. Commun*. **1998**, *244*, 253-257.
6. Henzler, K.W.; Lee, D.K.; Ramamoorhty, A. *Biochemstry*, **2003**, *42*, 6545-6558.
7. Moon, J.Y.; Henzler, K.W.; Ramamoorthy, A. *Biochim. Biophys. Acta*, **2006**, *1758*, 1351-1358.
8. Durr, U.H.N.; Sudheendra, U.S.; Ramamoorthy, A. *Biochim. Biophys. Acta*, **2006**, *1758*, 1408-1425.
9. K. Pütsep, G. Carlsson, H. Boman, M. Andersson, Lancet 360 (2005) 1144–1149.
10. Cirioni, O.; Giacometti, A.; Ghiselli, R.; Bergnach, C.; Orlando, F.; Silvestri, C.; Mocchegiani, F.; Licci, A.; Skerlavaj, B.; Rocchi, M.; Saba, V.; Zanetti, M.; Scalise, G. *Antimicrob. Agents Chemother*. **2006,** *50*, 1672-1679.
11. Oren, Z.; Lerman, J.C; Gudmundsson, G.H.; Agerberth, B.; Shai, Y. *J. Biochem*. **1999**, *341*, 501-513.

12. Henzler, K.W.; Martinez, G. V.; Brown, M.F.; Ramamoorthy, A. *Biochemistry*, **2004**, *43*, 8459-8469

13. Penumatcha, R. M.S. Thesis, Eastern Michigan University, Michigan, USA, 2007.

14. Turner, J.; Cho, Y.; Dinh, N.N.; Waring, A.J.; Lehrer, R.I. *Antimicrob Agents Chemother*, **1998**, *42(9),* 2206-2214. .

15. http://www.sigmaaldrich.com/Brands/Sigma_Genosys/Custom_Peptides/Key_Resources/Solid_Phase_Synthesis.html, (accessed September 30, 2007).

16. Nikolaus, D. U. H. PhD. Dissertation, University of Karlsruhe, Germany, 2005.